

RESEARCH ARTICLE

Effect of iron addition on mAb productivity and oxidative stress in Chinese hamster ovary culture

Ryan J. Graham¹ | Adil Mohammad² | George Liang¹ | Qiang Fu³ |
Bingyu Kuang¹ | Ashli Polanco¹ | Yong Suk Lee⁴ | R. Kenneth Marcus⁵  |
Seongkyu Yoon^{1,3} 

¹Department of Chemical Engineering, University of Massachusetts Lowell, Lowell, Massachusetts, USA

²Division of Product Quality Research, Office of Testing and Research, Office of Pharmaceutical Quality, Center for Drug Evaluation and Research, Food and Drug Administration, Silver Spring, Maryland, USA

³Department of Biomedical Engineering and Biotechnology, University of Massachusetts Lowell, Lowell, Massachusetts, USA

⁴Department of Biomedical and Nutritional Sciences, University of Massachusetts Lowell, Lowell, Massachusetts, USA

⁵Department of Chemistry, Clemson University, Clemson, South Carolina, USA

Correspondence

Seongkyu Yoon, Department of Chemical Engineering, University of Massachusetts Lowell, One University Avenue, Lowell, MA 01854, USA.

Email: seongkyu.yoon@uml.edu

Funding information

National Institute for Innovation in Manufacturing Biopharmaceuticals, Grant/Award Number: 70NANB17H002; National Science Foundation, Grant/Award Number: 1624718

Abstract

Trace metals play a critical role in the development of culture media used for the production of therapeutic proteins. Iron has been shown to enhance the productivity of monoclonal antibodies during Chinese hamster ovary (CHO) cell culture. However, the redox activity and pro-oxidant behavior of iron may also contribute toward the production of reactive oxygen species (ROS). In this work, we aim to clarify the influence of trace iron by examining the relationship between iron supplementation to culture media, mAb productivity and glycosylation, and oxidative stress interplay within the cell. Specifically, we assessed the impacts of iron supplementation on (a) mAb production and glycosylation; (b) mitochondria-generated free hydroxyl radicals (ROS); (c) the cells ability to store energy during oxidative phosphorylation; and (d) mitochondrial iron concentration. Upon the increase of iron at inoculation, CHO cells maintained a capacity to rebound from iron-induced viability lapses during exponential growth phase and improved mAb productivity and increased mAb galactosylation. Fluorescent labeling of the mitochondrial hydroxyl radical showed enhanced environments of oxidative stress upon iron supplementation. Additional labeling of active mitochondria indicated that, despite the enhanced production of ROS in the mitochondria, mitochondrial membrane potential was minimally impacted. By replicating iron treatments during seed train passaging, the CHO cells were observed to adapt to the shock of iron supplementation prior to inoculation. Results from these experiments demonstrate that CHO cells have the capacity to adapt to enhanced environments of oxidative stress and improve mAb productivity and mAb galactosylation with minimal perturbations to cell culture.

KEYWORDS

cell adaptation, CHO cell culture, iron supplementation, mAb glycosylation, mitochondrial membrane potential, oxidative stress

1 | INTRODUCTION

Trace metals are an integral component of Chinese hamster ovary (CHO) cell culture media employed for the production of therapeutic proteins. During the industrial production of monoclonal antibodies

(mAbs), key metals including zinc, copper, manganese, and iron are required as cofactors for a variety of intracellular demands to maximize the overall CHO cell culture performance.^{1–4} Efforts to further enhance mAb productivity and elicit desirable product quality profiles involve supplying trace metals to culture media in excess beyond basal provisions. For example, enhanced zinc supplementation has shown to increase mAb productivity,^{2,5} galactosylation,³ and suppress apoptosis⁶ and combat oxidative stress⁷ to prolong CHO culture. Copper supplementation can enhance the mAb productivity and induce lactate consumption and minimize waste metabolites.⁴ Additional manganese provisions have proven to be an effective process lever for managing glycosylation profiles.^{8,9} Iron supplementation has demonstrated enhanced cell growth and mAb titer.^{10,11}

While simultaneously enhancing mAb production under various metabolic, biosynthetic, and secretory pathways, trace metals also play a critical role in oxidative stress during cell culture. Oxidative stress occurs when an intracellular imbalance of antioxidants with free radicals and other reactive oxygen species (ROS) propagate a host of damaging modifications to proteins, enzymes, membranes, and DNA/RNA.^{12–14} Redox-active transition metals such as copper and iron are involved in a series of pathways responsible for ROS generation including free hydroxyl radical production via the Fenton and Haber–Weiss mechanisms.^{15,16} On the contrary, zinc serves as an antioxidant not only by stabilizing sulfhydryl residues prone to oxidation, but also as a cofactor for superoxide dismutase (SOD).¹⁷ With regard to product quality metrics, mAb glycosylation and other post-translational modifications occur in endoplasmic reticulum (ER), where ROS and ER stresses may have a significant impact on product quality characteristics such as glycan structure, disulfide bond formation, and amino acid oxidation.¹⁸ Recent reports have detailed the impact of these stresses on mitochondrial functionality and overall cell health both in CHO cells¹⁹ and other mammalian systems.²⁰ As mitochondria are a primary source of ROS propagation for the remainder of the cell,²¹ it is necessary to consider how mitochondrial ROS generation impacts post-translational modifications of hosted mAbs.

In CHO cell culture specifically, the cytotoxic responses to oxidative stress are generally manifested in mAb quality heterogeneity as well as lapses in cell growth and productivity.²² Efforts to mitigate the impact of oxidative stress have included supplementing culture media with stabilizing thiols^{23,24} and other ROS-scavenging compounds.²⁵ Trace metal supplementation strategies have also been employed for this purpose. For example, adding copper, manganese, and tryptophan to media have shown to decrease tryptophan oxidation of mAb products as well as upregulate oxidative stress-related genes to better control ROS within the cell.^{26,27} Copper supplementation has been employed as an online controller for redox potential,²⁸ and zinc supplementation has also shown to maintain SOD and peroxidase activity required for defending against oxidative stress.⁶ Trace metal chelation strategies have also been employed for managing cellular stress environments. For example, iron chelators such as EDTA and various polyamines have been supplied to maintain glycan consistency and improve cell growth.^{25,29,30} Whereas the average basal provision of copper (~15 μM), manganese (~0.45 μM), and zinc (~7.88 μM) in six

commercially-available CHO culture media showed minimal deviation, iron has been supplied in more bulk concentrations (~175.91 μM) with a wide range exceeding 400 μM .³¹ Further supplementation of iron provisions to CHO culture media beyond basal provisions have shown conflicting results. While some reports indicate that added supplements of iron anywhere from 100 to 500 μM can enhance CHO culture titer and improve cell growth,^{10,32} others have reported either no impact³³ or detriments to product quality profile under particular circumstances.¹¹ Thus, the degree to which available iron can enhance CHO culture performance without actuating enhanced intracellular stresses remains unclear.

In this work, we aimed to clarify the influence of trace iron on CHO culture performance by examining the relationship between iron provisions, mAb productivity and glycosylation, and oxidative stress interplay within the cell. Our experimental approach includes (1) culturing cells in culture media at 50, 100, 150, and 200 μM iron and observing the subsequent impact on cell growth and viability as well as mAb production and glycosylation; (2) identifying how these phenomena induce hydroxyl radical production within the mitochondria and furthermore modify mitochondrial functionality within the electron transport chain; and (3) characterizing the relatedness of intracellular and intramitochondrial availability of iron and zinc to ROS generation within the mitochondria. Concurrently, we further explore the cells' ability to acclimate to iron-induced stresses in efforts to achieve peak culture performance while pacifying the cellular environment from enhanced oxidative stress.

2 | MATERIALS AND METHODS

2.1 | Materials

A VRC01 CHO-K1 cell line hosting an IgG1 mAb was acquired from the National Institute of Health (NIH) and subsequently banked and maintained in liquid nitrogen prior to experimentation. AMBIC 1.1 Basal Medium (Lonza, Basel, Switzerland) was acquired through the Advanced Mammalian Biomanufacturing Innovation Center (AMBIC) and kept at 4°C prior to experimentation. L-glutamine (ThermoFisher Scientific, Waltham, MA) was maintained at –20°C and thawed at room temperature when needed. All sterile and non-sterile trace metal solutions (MilliporeSigma, St. Louis, MO) employed for culture media supplementation and analysis were maintained at room temperature. Sterile pipettes (VWR International, Radnor, PA), shake flasks (ThermoFisher Scientific), and centrifuge tubes (VWR International) were used for all experimentation herein. All reagents provided in the Mitochondria Isolation Kit for Cultured Cells (ThermoFisher Scientific), Pierce 660 nm Protein Assay Reagent (ThermoFisher Scientific), Mitochondrial Hydroxyl Radical Detection Assay Kit (Abcam, Cambridge, United Kingdom), and TMRE-Mitochondrial Membrane Potential Assay Kit (Abcam) were allocated and stored according to vendor instructions. The 96-well plates acquired for fluorescence detection were acquired from ThermoFisher Scientific. All other chemicals and reagents were acquired from MilliporeSigma unless otherwise noted.

Milli-Q water (MilliporeSigma) was used to prepare all reagents where needed.

2.2 | Cell culture operations and data acquisition

One vial of cells ($\sim 20^6$ cells) was thawed and seeded in AMBIC 1.1 Basal medium in a 125 mL shake flask. The seed culture was grown and expanded over 6 days in a Multitron incubator (Infors USA, Weymouth, MA) maintained at 37°C with orbital shaking at 125 RPM and a 5% CO₂ overhead. At inoculation, 12 × 500 mL shake flasks were supplied with 200 mL culture media supplemented with 8 mM glutamine and either 50, 100, 150, 200 μM Fe(NO₃)₃ · 9H₂O, along with a no-supplementation control ($n = 2$ each treatment) in addition to the basal provision. Cells were inoculated at $\sim 0.4 \times 10^6$ cells/mL and cultures were maintained in batch mode over a period of 7 days. Cell growth and viability were monitored each day via trypan blue exclusion using a Cedex Hi Res automated cell counter (Roche Holding AG, Basel, Switzerland). Additional supernatant aliquots were kept in 1.5 mL centrifuge tubes and stored at -20°C for subsequent analyses. Daily pellets of 2.5×10^6 cells were centrifuged at 300 RCF × 3 min in either a Sorvall Legend RT (ThermoFisher Scientific) or an Eppendorf centrifuge 5424 R (Eppendorf, Hamburg, Germany) depending on cell density, washed with ×1 PBS, and stored at -20°C for subsequent trace metal analysis.

On day 5, mitochondria from 80×10^6 cells were isolated using the Mitochondria Isolation Kit for Cultured Cells (ThermoFisher Scientific) according to vendor instructions. For each flask, 4 × pellets of 20×10^6 cells were spun down in an Eppendorf centrifuge 5424 R at 850 RCF × 2 min. Each pellet was resuspended in 800 μL of Reagent A, vortexed for 5 s, and incubated on ice for 2 min. Next, 10 μL of Reagent B were added to each tube and incubated on ice for 5 min with periodic vortexing in 1-min intervals. Eight hundred microliters of Reagent C was then added to each tube and inverted several times by hand prior to centrifugation at 700 RCF × 10 min at 4°C. After centrifugation, the supernatant was transferred to a new 2.0 mL centrifuge tube and re-centrifuged at 3000 RCF × 15 min at 4°C. The supernatant was carefully discarded without dislodging the mitochondria pellet, which was subsequently washed with 500 μL of Reagent C and centrifuged at 12,000 × 5 min. The supernatant was discarded, and the mitochondria pellet was stored at -20°C for subsequent trace metal analysis.

A subsequent seed train adaptation study was conducted to further explore the impact of iron provisions on culture performance. A series of three seed flasks were provided: control, 50, and 100 μM provisions of Fe(NO₃)₃ · 9H₂O. Each flask was passaged three times over a period of 8 days prior to inoculation with each respective iron-supplied media. Cells from seed flasks were used in a modified experimental design and provided these various concentrations of supplied Fe(NO₃)₃ · 9H₂O (18 flasks, $n = 2$ each treatment) and cultured in 50 mL volumes in 125 mL flasks. All cell culture maintenance and data acquisition activities were conducted as previously detailed.

2.3 | Mitochondrial hydroxyl radical production assay

On days 3 and 5 of the initial cell culture experiment, the mitochondrial hydroxyl radical was monitored utilizing the Mitochondrial Hydroxyl Radical Detection Assay Kit (Abcam). On a Corning poly-d-lysine coated 96-well plate (ThermoFisher Scientific), $\sim 0.25 \times 10^6$ cells/well were added in triplicates from each shake flask. The plate was centrifuged at 800 RPM × 2 min. Supernatants were decanted and 100 μL of ~ 0.6 OH580 probe diluted in assay buffer were added to each well without disrupting the pellet. Positive assay controls were treated with 10 μL of 0.1 M CuCl₂ and 10 μL of 1 M H₂O₂ in 1 × PBS (to undergo the Fenton reaction). After a 1-h incubation at 37°C, cell pellets were washed twice in 1 × PBS at 800 RPM × 2 min. After supernatants were removed, 100 μL of assay buffer was added to each well, and fluorescence was monitored at 540/590 Ex/Em with a 570 cutoff on a SpectraMax M2 (Molecular Devices, San Jose, CA) interfaced with SoftMax Pro 7.0.2 software (Molecular Devices) for data acquisition.

2.4 | Mitochondrial membrane potential assay

Mitochondrial membrane potential was also monitored on days 3 and 5 of the initial cell culture experiment using the TMRE-Mitochondrial Membrane Potential Assay Kit (Abcam). A sample of $\sim 0.75 \times 10^6$ cells were taken from each flask and placed in 1.5 mL centrifuge tubes. Cells were centrifuged at 300 RCF × 3 min and supernatants were carefully discarded. Each pellet was then resuspended in with 315 μL of 1 μM TMRE in culture media and incubated at 37°C for a half hour. Positive assay controls were treated with 20 μM of carbonyl cyanide 4-trifluoromethoxy phenylhydrazone (FCCP) to depolarize mitochondria and minimize membrane potential prior to incubation. After incubation, cells were washed in 0.2% bovine serum albumin (BSA) in ×1 PBS and resuspended in 315 μL of 0.2% BSA in ×1 PBS solution. Aliquots of 100 μL were added in triplicate wells on a 96-well plate and fluorescence was monitored at 549/575 Ex/Em with a 570 cutoff.

2.5 | mAb titer

Daily 1 mL cell culture supernatant samples were centrifuged at 10,000g for 10 min in the Eppendorf centrifuge 5424 R. mAb titer was quantified by Agilent 1100 high-performance liquid chromatography (HPLC) system (Agilent Technologies, Santa Clara, CA) coupled with a ultraviolet detector (UV) (Agilent Technologies) and a POROS® A 20 μm column (ThermoFisher Scientific). The mobile phase buffer consists of a binding buffer (50 mM sodium phosphate pH 7) and an elution buffer (100 mM sodium phosphate pH 2.3). The column was twice equilibrated at 20 × column length at a flow rate of 0.4 mL/min with both binding and elution buffers in an alternating pattern. For analysis, the column was gradually increased to 1.5 mL/min and

equilibrated with the starting condition for 20× column length set at 100% binding buffer. Subsequently, 20 µL of prepared sample was injected for analysis. Eluted samples were monitored for UV absorbance at 280 nm and referenced to a standard curve generated with IgG from human serum (MilliporeSigma) to determine mAb titer (g/L). All samples were run in duplicate measurement. Titers and cell counts were used to determine specific productivity (q_p) using a previously described method.¹¹

2.6 | mAb glycosylation

Daily 1 mL cell culture supernatant samples were centrifuged at 10,000g for 3 min to remove cell pellets and then purified using 20 µL of Pierce™ protein A/G agarose beads (ThermoFisher Scientific) coupled with a magnetic bead stand. The method consisted of a washing/binding buffer (50 mM sodium phosphate [pH 7]), elution buffer (100 mM sodium phosphate [pH 2.5]), and a neutralization buffer (500 mM sodium phosphate [pH 9]). The agarose beads were first preconditioned twice with 250 µL of binding buffer before adding in 1 mL of centrifuged supernatant samples. Samples were then incubated for 15 min on an Orbital shaker plate (IKA, Wilmington, NC) at 310 RPM/min. Subsequently, samples were washed twice with 500 µL of wash buffer, and once with 500 µL of MilliQ water. Fifty microliters of elution buffer was added to the bead solution and incubated on the shaker plate for 10 min at 310 RPM/min. The eluted samples were then placed in 1.5 mL centrifuge tubes containing 16 µL of neutralization buffer. The purified mAbs were quantified by Nanodrop™ OneC spectrophotometer (ThermoFisher Scientific) with a UV wavelength setting at 280 nm. Twenty micrograms of protein were denatured using denaturation buffer (New England Biolabs, Ipswich, MA) at 1× concentration and heated to 100°C for 10 min before cooling the samples on ice. mAb digestion was conducted by adding 3 µL of ×10 reaction buffer (New England Biolabs), 3 µL of NP-40 (New England Biolabs) and nanopure water were added to the samples to target a total reaction volume of 30 µL. 0.2 µL of PNGaseF enzyme (500,000 units/mL) (New England Biolabs) were added to the solution to digest the mAb at 37°C for 2 h. Twenty microliters of 2-AB labeling solution was added with 10 µL of solvent solution consisting of 70% DMSO (Sigma Aldrich, St. Louis, MO) and 30% Acetic Acid (Sigma Aldrich). The 2-AB labeling solution was made by dissolving 0.35 M 2-aminobenzamide and 1 M 2-picoline borane (Sigma Aldrich) in the solvent solution. The sample was then incubated at 65°C for 2.5 h. Excessive 2-AB labeling solution was removed through HyperSep Diol Cartridge (100 mg/mL) (ThermoFisher Scientific) with the use of a vacuum manifold (Waters, Milford, MA). Diol SPE cartridges were preconditioned with 1 mL of MilliQ water and 4 mL of acetonitrile (Sigma Aldrich) before sample loading. Samples were diluted with acetonitrile with a ratio of 1:9 and loaded into the preconditioned cartridges. The samples were then washed with two subsequent 500 µL of acetonitrile. Thereafter, the samples were eluted twice with 150 µL of MilliQ water and collected in 1.5 mL tubes. All flow throughs in the cartridge were controlled at a rate of 1 droplet/s.

The samples were then concentrated in a speed vacuum (ThermoFisher Scientific) at room temperature for 1.5 h to reach a final sample volume of 90 µL.

An Agilent 1100 HPLC system coupled with a fluorescence detector and Acquity UPLC BEH Glycan (HILIC column), 2.1 × 50 mm, 1.7 µm (Waters) were used to quantify the glycan profile. The mobile phase consisted of 100 mM ammonium formate (pH 4.5) and acetonitrile. The column was pre-equilibrated 20×column length at a flow rate of 0.1 mL/min with starting conditions of 75% 100 mM ammonium formate and 25% acetonitrile. The flow rate was gradually ramped up to 0.4 ml/min at the starting condition. Subsequently, 2 µL of sample were injected into the column. A gradient elution was used to elute the samples: 75% 100 mM ammonium formate to 65% over 15 min. The column was then reconditioned for 7 min at the starting condition to prepare for the next sample injection. The entire method was conducted at a flow rate of 0.4 mL/min. The fluorescence detector signal setup for excitation was 350 nm with a scan range of 220–380 nm in 5 nm incremental steps. Emission was acquired at 420 nm, with a scan range of 300–500 nm in 5 nm incremental steps. The temperature of the column was maintained at 50°C.

2.7 | Trace metal analysis

Trace metals were quantified in cell pellets on days 1, 3, and 5 as well as mitochondria pellets on day 5 by inductively coupled plasma mass spectrometry (ICP-MS). The analytical technique closely follows a previously described method.³¹ Briefly, a Perkin Elmer Nexlon 300D ICP-MS (Perkin Elmer, Waltham, MA) was complexed with a PrepFast-advanced automated dilution system (Elemental Scientific Inc, Omaha, NE) for zinc and iron analysis. First, calibration curves for zinc and iron were generated in triplicate measurements and referenced to an indium internal standard. Sample preparation involved thawing pellets of 2.5×10^6 live cells and 80×10^6 mitochondria at room temperature. Next, pellets were treated with 2 mL of 1% Triton-X 100 (%w/v) and vortexed for 1 h in 15-min intervals. Samples were centrifuged at 15,000 RCF for 10 min, and lysates were treated in 2% HNO₃ created with Optima grade nitric acid (ThermoFisher Scientific) according to the previously established method³¹ and loaded onto the PrepFast autosampler for analysis. Concentrations of iron and zinc as initially supplied in the AMBIC 1.1 basal media formulation are intentionally withheld from this manuscript.

3 | RESULTS

3.1 | Iron supplementation extends culture duration and enhances mAb specific productivity and galactosylation

Iron was added in 50, 100, 150, or 200 µM concentrations to examine the corresponding impact on CHO culture performance and to resolve

the relationships between mitochondrial oxidative stress, trace metal availability, and the ability of the cells to store energy. All cultures were run in batch mode to minimize metabolic waste accumulation which is known to introduce additional oxidative stresses to cell culture.²²

During lag-growth phase up through day 2, the control flasks grew $\sim 2\times$ faster than those supplied with excess iron and reached peak cell density at day 5 at 12.4×10^6 cells/mL (Figure 1(a)). Additionally, the control flasks maintained high viability greater than 99% through day 3 and greater than $\sim 95\%$ through day 5, after which the cultures experienced a rapid decline in viability (Figure 1(b)). In contrast, iron supplied flasks maintained a slower growth rate throughout the duration of the culture but experienced a prolonged growth period which peaked at day 6. On day 6, the 50 μM treatment peaked at 9.7×10^6 cells/mL, and 100, 150, and 200 μM treatments each peaked at $\sim 10.7 \times 10^6$ cells/mL, respectively (Figure 1(a)). After inoculation, all iron-treated cultures experienced an immediate decrease in viability, as 50 μM flasks dropped to 88% viability, and the remaining iron treatments fell to $\sim 76\%$ viability by day 2 (Figure 1(b)). However, throughout exponential growth phase by day 5, iron-treated cultures achieved similar viability to the control cultures at $\sim 95\%$ viability. Cell viabilities of 84% for the 50 μM treatment and 91% for the remaining

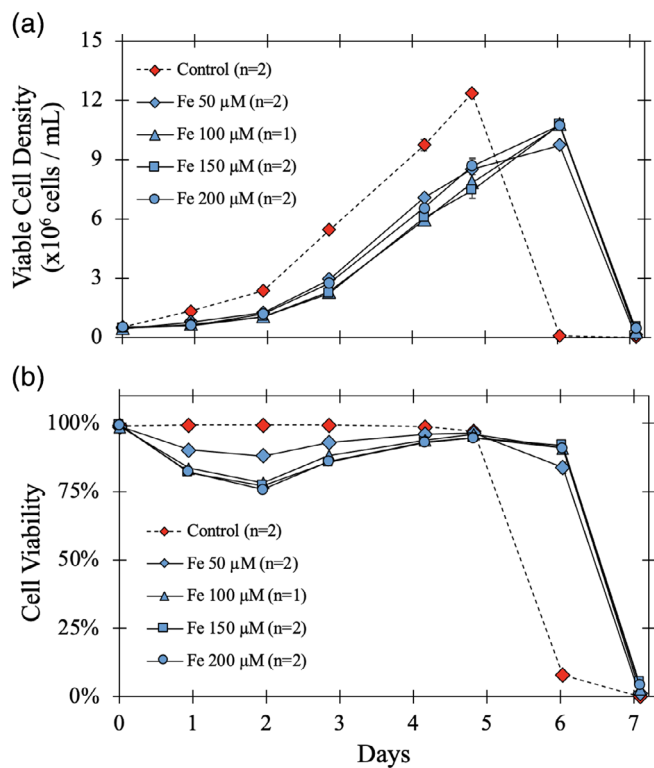


FIGURE 1 Chinese hamster ovary cell growth and viability of cultures treated with enhanced iron at inoculation. Error bars reflect half range of duplicate flask ($n = 2$ each treatment; $n = 1$ for 150 μM treatment due to contamination loss). (a) viable cell density ($p < 0.001$ for max VCD); (b) cell viability. Error bars for cell viability $< 1\%$ of measured value

iron treatments were maintained through day 6 before declining by the harvest day 7.

mAb titer was determined on days 5 and 6 where cultures achieved peak cell growth. However, all conditions achieved peak titer on day 6. On day 6, the control flasks achieved highest performance at 0.26 g/L, slightly outperforming the iron treated flasks which achieved lower peak titer at ~ 0.24 g/L (Figure 2(a)). However, iron-treated cultures achieved a higher specific production (q_p) through both days 5 and 6 (Figure 2(b)). Through day 5, the 50 μM iron supplemented flasks maintained the highest q_p , peaking at 12 pg/cell/

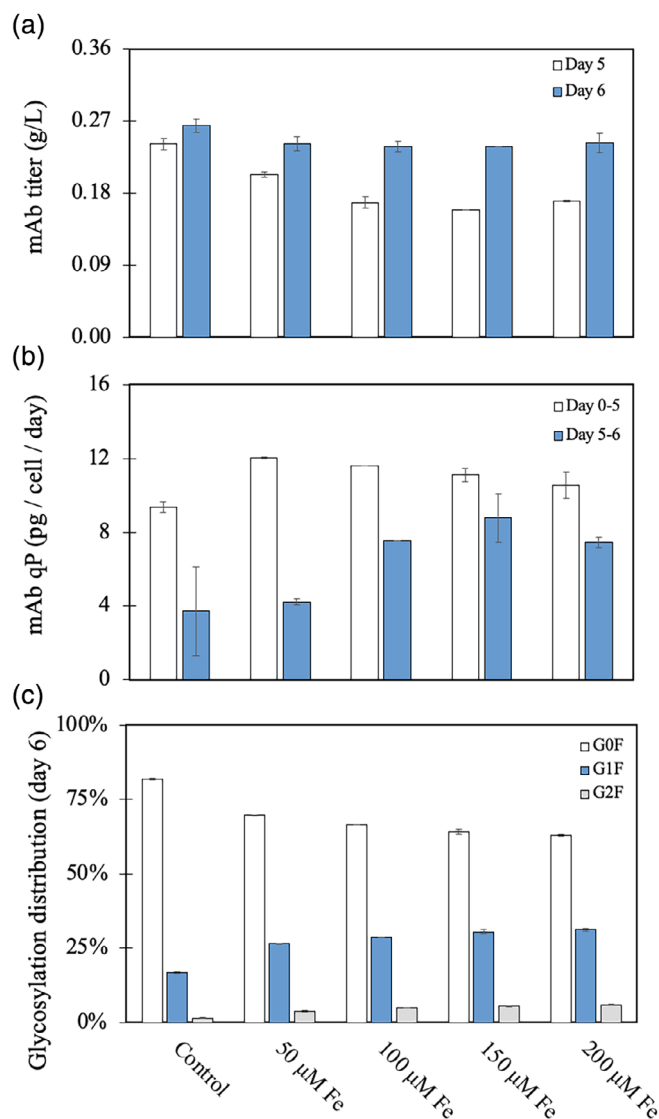


FIGURE 2 Chinese hamster ovary culture performance at peak cell growth. mAb titer, specific production (q_p), and glycosylation distribution. Analysis demonstrates overall culture mAb production as well as mAb production per cell hour. (a) mAb titer at peak cell growth day 5 ($p < 0.0000001$) and day 6 ($p < 0.01$); (b) mAb q_p at peak cell growth days 0–5 ($p < 0.0001$) and 5–6 ($p < 0.001$). (c) mAb glycosylation conformation at day 6 of G0F ($p < 0.00001$), G1F ($p < 0.00000001$), and G2F ($p < 0.00000001$). Error bars reflect half range of duplicate flask ($n = 2$ each treatment; $n = 1$ for 150 μM treatment due to contamination loss)

day, or $\sim 22\%$ higher than the control conditions. However, when considering q_p from day 5 through day 6, when iron supplemented cultures experienced a prolonged 24 h of high cell viability, the q_p for 100, 150, and 200 μM iron supplemented cultures remained high at greater than 7.5 pg/cell/day, whereas all other cultures remain at approximately 4 pg/cell/day.

Increased galactosylation was also observed in iron-treated flasks in a dose-dependent manner. On day 6, non-galactosylated GOF species accounted for $\sim 82\%$ of the observable glycan distribution in the control cultures, whereas the 50 μM iron treated flasks maintained only 70% of non-galactosylated species (all error bars for non-galactosylated species $< 0.5\%$) (Figure 2(c)). Non-galactosylated species decreased in stepwise manner for the remaining iron treatments, as the 100, 150, and 200 μM conditions are accounted for by $\sim 67\%$, $\sim 64\%$, and $\sim 63\%$ non-galactosylated species, respectively. These distributions also are similar to those on day 5 when control cultures are at peak cell density during stationary phase (Figure S1), offering that the presence of additional iron increased galactosylation throughout the duration of the culture.

3.2 | Enhanced iron induces mitochondrial oxidative stresses without altering mitochondrial membrane potential

The mitochondrial hydroxyl radical was assayed to assess the impact of enhanced iron supplementation on mitochondrial oxidative stress. During exponential growth phase on day 3, as iron-supplemented cultures began recovery from the sudden viability drop, hydroxyl radical presence in 100 and 200 μM iron treatments peaked at ~ 43 relative fluorescence units (RFU), while the 150 μM treatment eclipsed 49 RFU (Figure 3). Comparatively, the control and 50 μM iron treated cultures maintained hydroxyl radical content at less than 28.3 RFU, a drop of $\sim 40\%$ compared to the higher iron treated cultures. On day

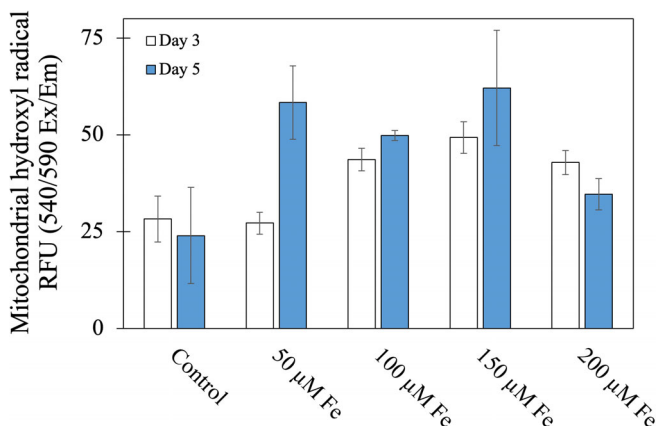


FIGURE 3 Mitochondrial hydroxyl radical content. Cultures assayed at day 3 (exponential growth phase, $p < 0.0001$) and day 5 (stationary phase, $p < 0.01$). Error bars reflect half range of duplicate flask ($n = 2$ each treatment; $n = 1$ for 150 μM treatment due to contamination loss)

5, the 50 μM iron treatment more than doubled from its day 3 value up to about ~ 58 RFU, pointing to a continued increase in hydroxyl radical production throughout the remainder of the culture. Similarly, the 100 and 150 μM iron treatments experienced a small increase in hydroxyl radical content by $\sim 16\%$ and $\sim 26\%$, respectively. The control cultures experienced only a small decrease in hydroxyl radical content from their day 3 value pointing to a more consistent mitochondrial ROS production throughout the culture duration.

Mitochondrial membrane potential was monitored on both days 3 and 5 to investigate the relationship of oxidative stress to the cells' ability to produce and store energy during oxidative phosphorylation (Figure 4). During exponential growth phase on day 3, the iron supplied flasks achieved a membrane potential $\sim 10\%$ higher than the control flask, with all flasks except the 100 μM treated flask exceeding a membrane potential of the control (Figure 4). By stationary phase at day 5, the iron treated flasks maintained a membrane potential increase of only $\sim 2\%$ on average compared to the control flasks, with the 50 and 100 μM treatments experiencing a slight decrease from the day 3 value and the 150 and 200 μM treatments showed a slight increase. This decrease from day 3 to 5 demonstrates minimal difference in membrane potential alongside increasing hydroxyl radical presence within the same timeframe from exponential growth through to stationary phase.

3.3 | Intracellular and intramitochondrial iron increases with media supplementation alongside enhanced oxidative stress

On days 1, 3, and 5, intracellular iron was monitored to understand the impact of enhanced media supplementation on cellular availability. Because zinc, an antioxidant, is responsible for mediating several anti-oxidation mechanisms within the cell, intracellular zinc was also surveyed. On day 1, intracellular iron was determined at 0.35, 0.40, and

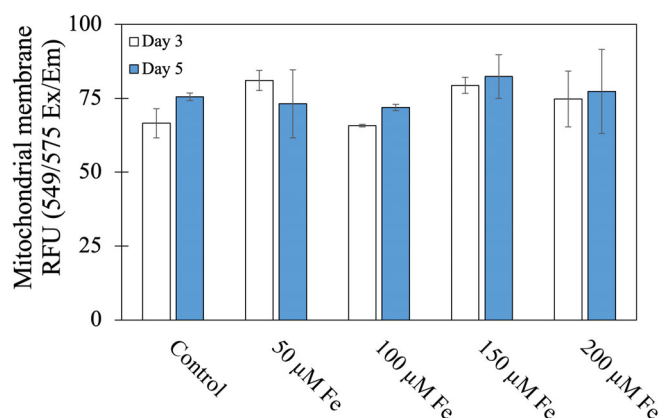


FIGURE 4 Mitochondrial membrane potential (ψ). Cultures assayed at day 3 (exponential growth phase, $p < 0.023$) and day 5 (peak VCD, $p < 0.61$). Error bars reflect half range of duplicate flask ($n = 2$ each treatment; $n = 1$ for 150 μM treatment due to contamination loss)

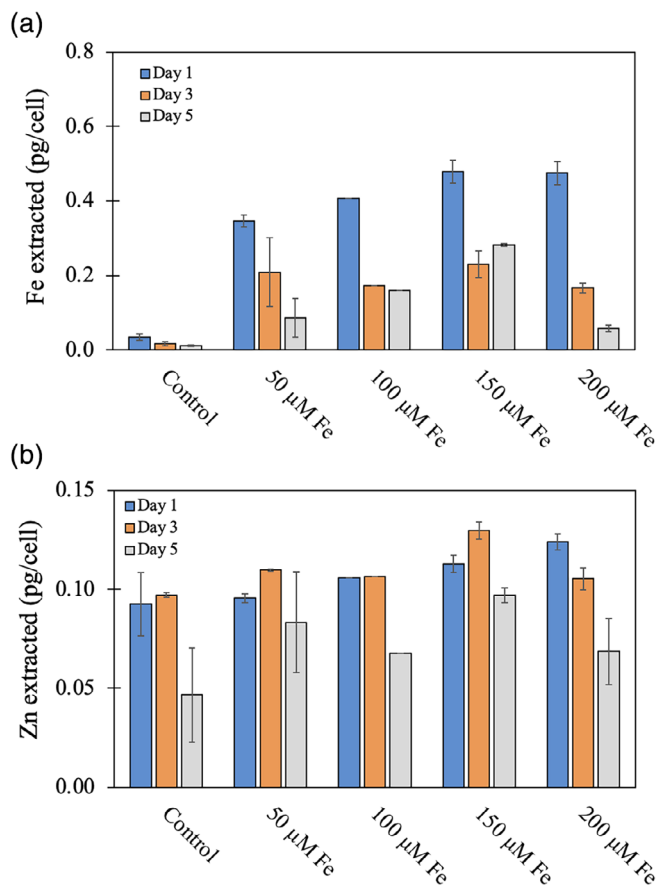


FIGURE 5 Intracellular iron and zinc content on days 1, 3, and 5. Results normalized to the mass of iron and zinc extracted from a single cell. All measurements conducted in biological duplicates (100 μM Fe $n = 1$ due to contamination); (a) intracellular iron on days 1 ($p < 0.0003$), 3 ($p < 0.061$), and 5 ($p < 0.003$); (b) intracellular zinc on days 1 ($p < 0.09$), 3, ($p < 0.005$), and 5 ($p < 0.29$). Error bars reflect half range of duplicate flask ($n = 2$ each treatment; $n = 1$ for 150 μM treatment due to contamination loss)

0.47 pg/cell extracted in the 50, 100, and 150–200 μM Fe supplied flasks, confirming that enhanced media supplementation of iron to culture media is transported into the cell (Figure 5(a)). During exponential growth and stationary phase on days 3 and 5, the amount of available iron within the cell decreased by more than 50% of each condition's respective day 1 value. Also, on day 1, intracellular zinc increases alongside increased iron in stepwise manner, ranging from 0.093 up to 0.124 pg / cell in 1 mL lysate in all five conditions (Figure 5(b)). On day 3, available zinc fell within ~20% of the day 1 availability, with the control, 50 μM, and 100 μM conditions slightly higher than their day 1 value, and the 150 and 200 μM conditions slightly lower. By day 5, intracellular zinc fell ~50% of the day 3 value for each condition.

On day 5, mitochondrial iron and zinc availability were both measured in order to characterize the relationship between pro-oxidant/antioxidant metals and oxidative stress within the mitochondria. Mitochondrial iron increased stepwise from the control to each of the four iron conditions, starting at 0.001 pg/mitochondria extracted (control

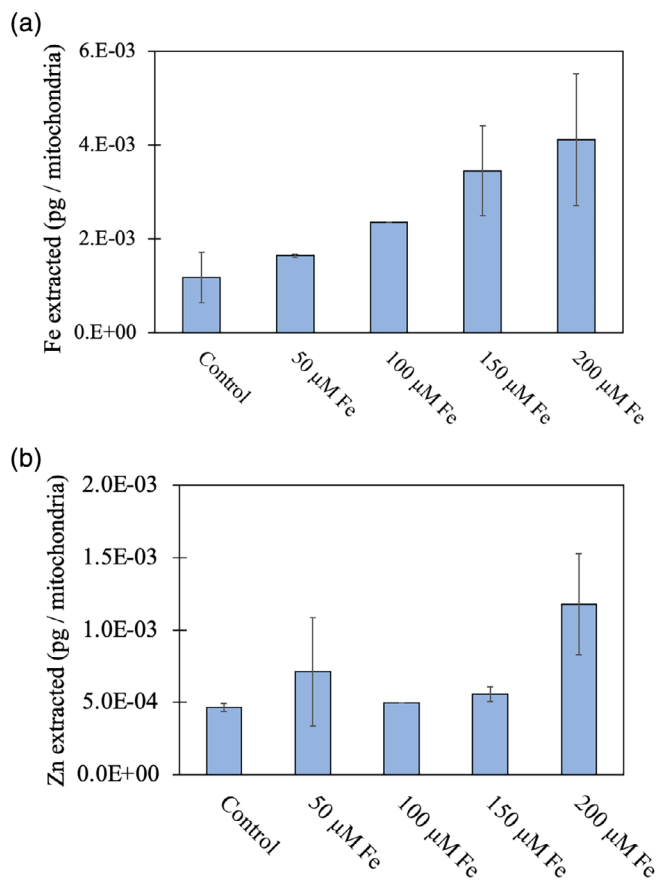


FIGURE 6 Intra-mitochondrial iron and zinc content on day 5. Results normalized to the mass of iron or zinc extracted from mitochondria which were extracted from 80×10^6 live cells lysed with 1 mL of 1% Triton-X 100 (%1/v). All measurements conducted in biological duplicates (100 μM Fe $n = 1$ due to contamination). (a) intra-mitochondrial iron on day 5 ($p < 0.12$); (b) intracellular zinc on day 5 ($p < 0.21$). Error bars reflect half range of duplicate flask ($n = 2$ each treatment; $n = 1$ for 150 μM treatment due to contamination loss)

condition) to 0.004 pg/mitochondria extracted (200 μM condition) (Figure 6(a)). Comparatively, mitochondrial zinc was less patterned and ranged from 0.0005 to 0.001 pg/mitochondria extracted for all conditions tested (Figure 6(b)). Because the relationship between pro-oxidant and antioxidant metals may be related to the produced hydroxyl radical by the Fenton mechanism, the ratio of iron to zinc within the mitochondria was observed alongside mitochondrial hydroxyl radical content (Figure 7). With the exception of the 50 μM condition which maintained a low iron to zinc ratio but high hydroxyl radical production, the other four conditions showed a proportional relationship between the iron to zinc ratio and the produced hydroxyl radical. Beginning with the control, followed by the 200, 100, and 150 μM conditions, more hydroxyl radical production coincided with a greater mitochondrial iron to zinc ratio. Here, the pro-oxidant versus antioxidant metal affinity within the mitochondria may point to a relatedness between metal availability and ROS generated within the mitochondria.

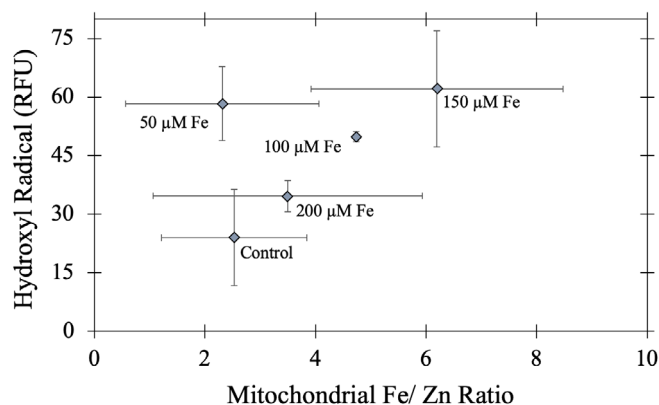


FIGURE 7 Mitochondrial hydroxyl radical versus mitochondrial Fe/Zn ratio on day 5. Figure demonstrates the relationship of oxidative stress to pro-oxidant/antioxidant trace metal availability within the mitochondria. Error bars along x-axis represent the average extrema of standard deviation from both Fe and Zn mitochondria metal measurements

3.4 | CHO cells adapt to high iron during seed train passaging to maximize growth and productivity during cell culture

An orthogonal study was conducted to determine the impact of iron adaptation during seed train passaging on cell culture performance. Two days after vial thawing, the initial seed flask was split into three conditions: control, 50 μM iron, and 100 μM iron and passaged every 2 days for a total period of 8 days. During the first adaptation cycle (days 2–4), the control flask significantly outgrew the 50 μM and 100 μM treated flasks, at 2.51×10^6 viable cells/mL compared to 1.48 and 1.27×10^6 viable cells/mL, respectively (Figure 8(a)). Also, within the first adaptation cycle, the control flask also maintained a higher percentage of viable cells at 99% viability compared to the 50 and 100 μM treatments which were determined to be 93% and 89% viable, respectively (Figure 8(b)). However, both viable cell density and cell viability of each of the three seed flasks continue to converge by the end of the third adaptation cycle (day 8), with the control flask, 50 μM flask, and 100 μM flask reaching viable cell densities of 2.7 , 2.5 , and 2.4×10^6 viable cells/mL at viabilities of 99.4%, 98.5%, and 97.8%, respectively.

Using cells from these three seed flasks at the end of the third adaptation cycle (day 8), a cell culture experiment was conducted wherein cells from each of the three flasks were treated with a comparable level of additional iron at either control, 50 μM , or 100 μM supplementations at inoculation ($n = 9$, each condition duplicated) (Figure 9(a)). Peak cell growth among all conditions from the control and 50 μM seed flasks were similar on day 5, where the best performing condition (1–1; control seeded cells cultured at control conditions) peaked at 12.24×10^6 viable cells/mL and the weakest performing condition (2–3; 50 μM seeded cells cultured in 100 μM iron) peaked at 10.59×10^6 viable cells/mL (Figure 9(b)). Throughout exponential growth phase, all cultures maintained $\sim 99\%$ viability with the exception

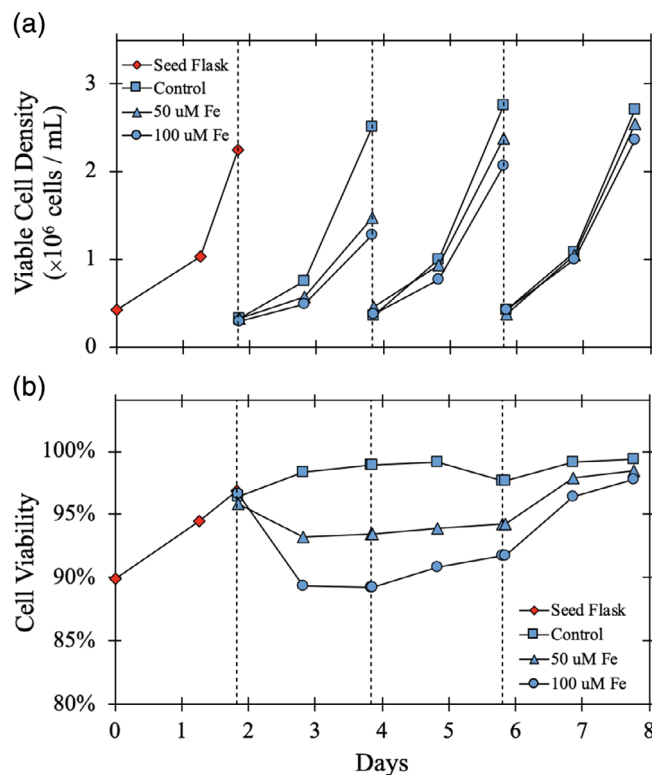


FIGURE 8 Cell growth and viability of seed train flasks provided with enhanced iron. Cells were passaged for 8 days in either control, 50, or 100 μM iron conditions; (a) viable cell density; (b) cell viability. Replicate flasks not used during seed train adaptation

of conditions 1–2 and 1–3 (control seeded cells cultured in both 50 and 100 μM iron), which were $\sim 96\%$ – 98% viable (Figure 9(c)). By stationary phase at day 5, as cultures began to descend into death phase, the control seeded cultures (1, 2, and 1–3) were slightly more viable than the 50 μM seeded cultures (2–1, 2–2, and 2–3) at $\sim 94\%$ – 95% viable. Cell growth and viability from the 100 μM seed flask trended very similar to those from the 50 μM seed flask, are shown as Supporting information for convenience (Figure S2). At peak cell growth on day 5, mAb titer was the highest for conditions 1–1 and 2–1, and 3–1 at 0.144, 0.142, and 0.138 g/L, respectively, which were seeded at, control, 50, and 100 μM iron but cultured in control conditions (Table 1). Conditions 2–2 and 3–3 were seeded and cultured at identical iron provisions (50 and 100 μM) and achieved titers of 0.137 and 0.132 g/L, respectively, outperforming treatments 1–2 and 1–3 which were only provided enhanced iron at the culture inoculation. These results indicate that seeding cells in high iron but culturing in smaller concentrations of iron have a positive impact on cell viability compared to only providing excess iron at inoculation.

4 | DISCUSSION

Trace metal content in culture media has a critical impact on the production of therapeutic proteins. Previously, iron supplementation to

CHO culture media have demonstrated favorable mAb production characteristics.^{10,11} However, as a major contributor to the cellular respiration pathways, iron supplementation may also have significant

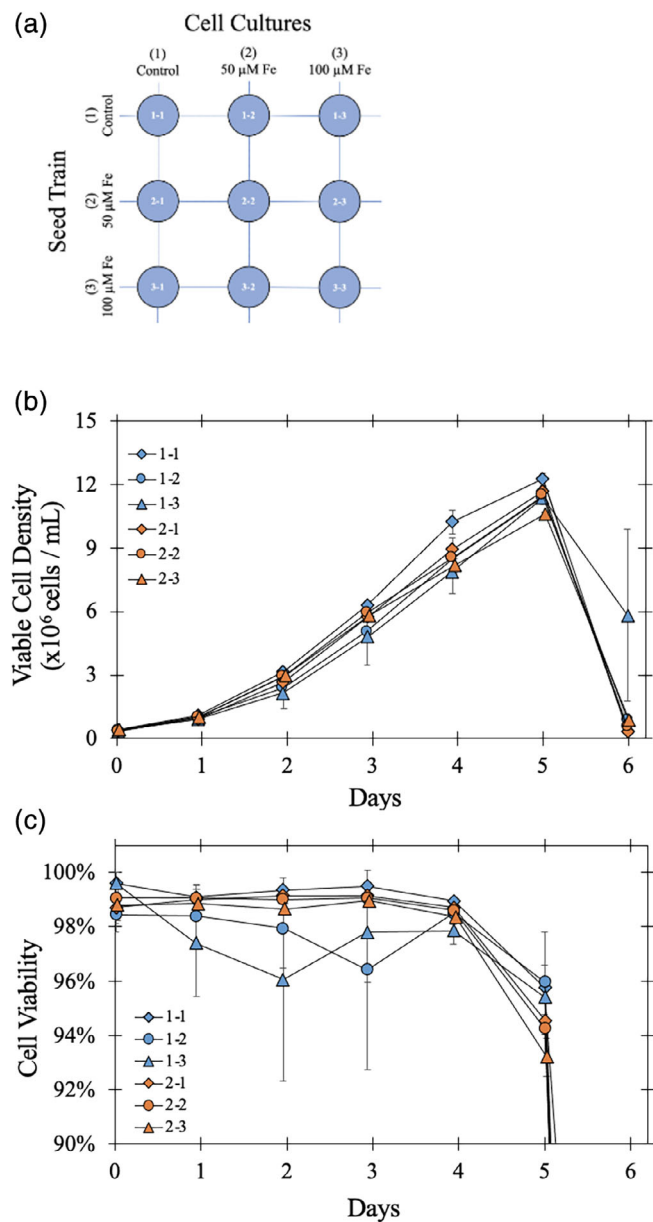


FIGURE 9 Cell growth and viability of cultures seeded with iron-adapted cells. (a) cell culture strategy from seed train adaptation with either control or 50, or 100 μM iron conditions; (b) viable cell density; (c) cell viability. All cell cultures run in duplicate flasks. Conditions 3-1, 3-2, and 3-3 are shown in Figure S2a,b

TABLE 1 mAb titer of cultures seeded with iron-adapted cells at peak cell growth day 5 (units in g/L)

		Cell culture		
		(1) Control	(2) 50 μM	(3) 100 μM
Seed train	(1) Control	0.144 (± 0.001)	0.136 (± 0.000)	0.125 (± 0.001)
	(2) 50 μM	0.142 (± 0.000)	0.137 (± 0.001)	0.108 (± 0.022)
	(3) 100 μM	0.138 (± 0.001)	0.134 (± 0.001)	0.132 (± 0.001)

Note: All cell cultures run in duplicate flasks. All titer values measured in technical duplicates.

consequences on oxidative stress within the mitochondria including the cellular ability to store energy during oxidative phosphorylation.^{22,34}

Metabolic waste accumulation as well as additional glucose have both been shown to induce oxidative stresses to cell culture.^{22,35,36} Therefore, to eliminate additional sources of ROS generation, the control, 50, 100, 150, and 200 μM iron treatments were all cultured in batch mode. Hence, lower cell growth and titer was anticipated as typical for batch mode culture. The control cultures achieved peak viable cell density during stationary phase at greater than $\sim 1.5 \times 10^6$ viable cells/mL compared to the iron treated flasks (12.4 vs. 10.7×10^6 viable cells/mL) yet achieved an overall titer only slightly higher than the iron treated flasks (Figures 1 and 2). The lapse in viability of the iron treated flasks can likely be attributed to an iron shock at inoculation which caused a 2-day viability lapse which cells recovered from as they reached stationary phase. Despite this lapse in viability, the iron treatments did enhance specific productivity both from day 0 to 5 as well as day 5-6 compared to the control (Figure 2(b)). Moreover, the iron treatments also impacted the mAb glycosylation pattern, as galactosylation increased along with each additional iron supplement (Figure 2(c)). Enhanced galactosylation has previously been shown to increase both complement-dependent cytotoxicity³⁷ and antibody-dependent cell-mediated cytotoxicity,³⁸ and is oftentimes a critical quality attribute during mAb production.³⁹ Additional provisions of uridine, galactose, and manganese have shown to increase galactosylation in mAbs.^{3,40,41} Our results herein demonstrate that iron supplementation may also be used to enhance or modulate galactosylation in therapeutic proteins.

Mitochondria are responsible for a myriad of key cellular processes including cell respiration, energy production and storage, cell signaling, and cell growth and lifecycle.⁴² Mitochondria also play a critical role in oxidative stress metabolism, maintain at least 10 different sites of ROS production while also contributing significantly to the antioxidation network throughout the cell.⁴³ During exponential growth phase (day 3), all iron supplied flasks experienced mitochondrial hydroxyl radical presence higher than the control with the exception of the 50 μM condition which was comparable to the control flask (Figure 3). However, by stationary phase (day 5), all iron supplied flasks maintained significantly higher hydroxyl radical than the control. Specifically, the 50, 100, and 150 μM conditions had more than double the hydroxyl radical than the control. These results point to enhanced mitochondrial oxidative stress with iron supplementation. Because iron is known to help generate the hydroxyl radical via the Fenton mechanism,^{15,16,44} it is likely that the iron supplementation increased reactions via this pathway, subsequently leading to the

lapses in cell viability. Despite enhanced oxidative stress environments caused by iron supplementation, the cells' ability to store energy during oxidative phosphorylation via mitochondrial membrane potential analysis was minimally impacted (Figure 4). Although peak mitochondrial functionality is tied to membrane potential, "optimal values" of membrane potential are unclear, as conditions of high membrane potential can significantly enhance ROS production within the mitochondria.⁴⁵ Mitochondrial membrane potential has previously been associated with peak cell production⁴⁶ as well as minimized lactate formation rates⁴⁷ in CHO cell culture. However, limited examinations into the specific relationships of mitochondrial membrane potential to oxidative stress were assessed in this work.

Intracellular iron concentrations increased upon media supplementation from the 50 μ M treatment up through the 150 μ M treatment, after which intracellular iron concentration plateaued (Figure 5(a)). Although not supplemented to culture media, intracellular zinc content also increased with stepwise iron supplementation from the 50 μ M treatment up through the 200 μ M treatment (Figure 5(b)), suggesting a possible relationship between related behavior of both metals in cell culture as previously reported.⁶ During stationary phase (day 5), intramitochondrial iron content also increased in stepwise manner with media supplementation for all treatments (Figure 6(a)), while intramitochondrial zinc appeared to have no decipherable trend (Figure 6(b)). Iron and zinc both play critical roles in oxidative stress interplay throughout the cell, both as pro-oxidant (free iron) and antioxidant (free zinc).^{1,13,22,48} Thus, mitochondrial iron and zinc can have opposite impact on the production of ROS within the mitochondria, specifically in free-ion form. Here, the ratio of total mitochondrial iron to zinc showed some relatedness to mitochondrial hydroxyl radical production. The control, 200, 100, and 150 μ M conditions showed a proportional relationship of intramitochondrial iron to zinc, as the metal ratio increased proportionally with hydroxyl radical production (Figure 7). However, the 50 μ M iron supplied flask did not follow this trend, as it maintained a low ratio of mitochondrial iron to zinc yet a high production of hydroxyl radical. This was likely attributed to the higher concentrations of mitochondrial zinc determined from both 50 μ M iron supplied flasks. Although these results point to an iron-zinc relatedness to oxidative stress within the mitochondria which falls in line with pro-oxidant/antioxidant interplay, a more thorough examination of the specific transporters and mechanisms of metal delivery to the mitochondria alongside varying conditions of oxidative stress would be required to expand any further on this hypothesis.

To eliminate the drop and recovery of cell viability upon iron supplementation at inoculation (Figure 1), cells demonstrated an ability to adapt to iron supplementation during seed train passaging (Figure 8). Passaging CHO cells in low iron environments has previously proven favorable toward improving titer without compromising drug substance color, even during enhanced intracellular ROS production.¹¹ Here, we demonstrate that passaging cells in high iron can significantly minimize the lapse in viability that would otherwise occur after inoculation. Similarly, this adaptation showed that passaging cells in high iron and culturing at control conditions shows an improvement in overall titer compared to supplying iron only at inoculation. The

phenomena of cell adaptation has been explored previously for adaptation to protein free media and corresponding transcriptomic changes have been characterized^{49,50} Transcriptomic and metabolic analysis of CHO cultures adapted to high-iron/oxidative stress environments would lend insight into the specific mechanisms responsible for adaptation and could subsequently be used for additional media optimization efforts.

Although these treatments did not demonstrate considerable increases in titer compared to the control condition 1-1, these approaches may be favorable for minimizing oxidative stress and maximizing galactosylation and other quality metrics shown here and elsewhere.¹¹ It also needs to be considered that although the iron seeding adaptation was specifically employed for adapting cells to iron-induced oxidative stress, the seed train for the initial cell culture run was employed solely for generating enough cells for inoculation which required a larger seeding volume of cells. Consequently, conditions 1-1, 1-2, and 1-3 in the seed train adaptation run did not experience a viability drop as significant as identically treated cultures in the first culture run. During the initial seed train, cells underwent daily passaging and expansion into larger culture volumes over a 6-day period until the required number of cells was available to inoculate the cell culture experiment. During the second seed train for adaptation, cells were routinely discarded after each adaptation cycle during the 8-day seed train and maintained at the lower densities required for the subsequent inoculation. While these differences are likely the cause for the discrepancies noticed, further investigation of seed train comparability would be required to assess this influence on cell culture.

5 | CONCLUSION

Herein, we have demonstrated that iron supplementation to CHO culture can improve productivity and galactosylation of an IgG mAb despite enhanced environments of oxidative stress generated within the mitochondria. Also, we have shown that cells can adapt to enhanced environments of oxidative stress induced by pro-oxidant trace metal availability within the mitochondria without negatively impacting the cells' ability to store energy. These efforts help to further the general understanding of the expansive role of trace metals on production of therapeutic proteins to maximize the performance of CHO cell culture. Because these mechanisms of oxidative stress and glycosylation are consistent across many mammalian cell types, we expect these results to be transferrable to other mAb-expressing CHO-K1 cell lines and production platforms (e.g., fed-batch and perfusion modes).

ACKNOWLEDGMENTS

The authors thank Professor Shannon Kelleher from the Biomedical & Nutritional Sciences Department at UMass Lowell for her guidance and insight into examining the impact of trace metals on oxidative stress. The authors also thank Annie Gagnon and Jack Lepine for their assistance with sample preparation for oxidative stress and membrane potential analyses, as well as Dr. Namjoon Kim for his guidance in the

laboratory for all tasks described herein. This project was funded in part by The National Institute for Innovation in Manufacturing Biopharmaceuticals (NIIMBL), Grant/Award Number: 70NANB17H002; National Science Foundation, Grant/Award Number: 1624718.

CONFLICT OF INTEREST

The authors declare that they have no known competing financial interests or personal relationships that could have appeared to influence the work reported in this paper.

PEER REVIEW

The peer review history for this article is available at <https://publons.com/publon/10.1002/btpr.3181>.

DATA AVAILABILITY STATEMENT

Data available on request from the authors.

ORCID

R. Kenneth Marcus  <https://orcid.org/0000-0003-4276-5805>

Seongkyu Yoon  <https://orcid.org/0000-0002-5330-8784>

REFERENCES

- Graham RJ, Bhatia H, Yoon S. Consequences of trace metal variability and supplementation on Chinese hamster ovary (CHO) cell culture performance: a review of key mechanisms and considerations. *Biotechnol Bioeng*. 2019;116:3446-3456.
- Kim BG, Park HW. High zinc ion supplementation of more than 30 μ M can increase monoclonal antibody production in recombinant Chinese hamster ovary DG44 cell culture. *Appl Microbiol Biotechnol*. 2016;100(5):2163-2170.
- Prabhu A, Gadre R, Gadgil M. Zinc supplementation decreases galactosylation of recombinant IgG in CHO cells. *Appl Microbiol Biotechnol*. 2018;102(14):5989-5999.
- Yuk IH, Russell S, Tang Y, et al. Effects of copper on CHO cells: cellular requirements and product quality considerations. *Biotechnol Prog*. 2015;31(1):226-238.
- Capella Roca B, Alarcon Miguez A, Keenan J, et al. Zinc supplementation increases protein titer of recombinant CHO cells. *Cytotechnology*. 2019;71(5):915-924.
- Graham RJ, Ketcham S, Mohammad A, et al. Zinc supplementation improves the harvest purity of beta-glucuronidase from CHO cell culture by suppressing apoptosis. *Appl Microbiol Biotechnol*. 2020;104(3):1097-1108.
- Graham RJ, Ketcham SA, Mohammad A, et al. Zinc supplementation modulates intracellular metal uptake and oxidative stress defense mechanisms in CHO cell cultures. *Biochem Eng J*. 2021;169:107928.
- Villiger TK, Roulet A, Perilleux A, et al. Controlling the time evolution of mAb N-linked glycosylation, part I: microbioreactor experiments. *Biotechnol Prog*. 2016;32(5):1123-1134.
- St Amand MM, Radhakrishnan D, Robinson AS, Ogunnaike BA. Identification of manipulated variables for a glycosylation control strategy. *Biotechnol Bioeng*. 2014;111(10):1957-1970.
- Bai Y, Wu C, Zhao J, Liu YH, Ding W, Ling WL. Role of iron and sodium citrate in animal protein-free CHO cell culture medium on cell growth and monoclonal antibody production. *Biotechnol Prog*. 2011;27(1):209-219.
- Xu J, Rehmann MS, Xu X, et al. Improving titer while maintaining quality of final formulated drug substance via optimization of CHO cell culture conditions in low-iron chemically defined media. *mAbs*. 2018;10(3):488-499.
- Halliwell B. Cell culture, oxidative stress, and antioxidants: avoiding pitfalls. *Biom J*. 2014;37(3):99-105.
- Halliwell B. Oxidative stress in cell culture: an under-appreciated problem? *FEBS Lett*. 2003;540(1-3):3-6.
- Kong Q, Lin CL. Oxidative damage to RNA: mechanisms, consequences, and diseases. *Cell Mol Life Sci*. 2010;67(11):1817-1829.
- Jomova K, Baros S, Valko M. Redox active metal-induced oxidative stress in biological systems. *Transition Met Chem*. 2012;37(2):127-134.
- Winterbourn CC. Toxicity of iron and hydrogen peroxide: the Fenton reaction. *Toxicology Lett*. 1995;82-83:969-974.
- Eide DJ. The oxidative stress of zinc deficiency. *Metallomics: Integr Biomet Sci*. 2011;3(11):1124-1129.
- Zeeshan HMA, Lee GH, Kim H-R, Chae H-J. Endoplasmic reticulum stress and associated ROS. *Int J Mol Sci*. 2016;17(3):327-327.
- Ali AS, Chen R, Raju R, et al. Multi-Omics reveals impact of cysteine feed concentration and resulting redox imbalance on cellular energy metabolism and specific productivity in CHO cell bioprocessing. *Biotechnol J*. 2020;15:1900565.
- Burgos-Moron E, Abad-Jimenez Z, Maranon AM, et al. Relationship between oxidative stress, ER stress, and inflammation in type 2 diabetes: the Battle continues. *J Clin Med*. 2019;8(9):1385.
- Kuznetsov AV, Kehrer I, Kozlov AV, et al. Mitochondrial ROS production under cellular stress: comparison of different detection methods. *Anal Bioanal Chem*. 2011;400(8):2383-2390.
- Chevallier V, Andersen MR, Malphettes L. Oxidative stress-alleviating strategies to improve recombinant protein production in CHO cells. *Biotechnol Bioeng*. 2020;117(4):1172-1186.
- Yun Z, Takagi M, Yoshida T. Effect of antioxidants on the apoptosis of CHO cells and production of tissue plasminogen activator in suspension culture. *J Biosci Bioeng*. 2001;91(6):581-585.
- Kuschelewski J, Schnellbaecher A, Pering S, Wehling M, Zimmer A. Antioxidant effect of thiazolidine molecules in cell culture media improves stability and performance. *Biotechnol Prog*. 2017;33(3):759-770.
- Gaboriau F, Kreder A, Clavreul N, Moulinoux J-P, Delcros J-G, Lescoat G. Polyamine modulation of iron uptake in CHO cells. *Biochem Pharmacol*. 2004;67(9):1629-1637.
- Hazeltine LB, Knueven KM, Zhang Y, Lian Z, Olson DJ, Ouyang A. Chemically defined media modifications to lower tryptophan oxidation of biopharmaceuticals. *Biotechnol Prog*. 2016;32(1):178-188.
- He L, Desai JX, Gao J, et al. Elucidating the impact of CHO cell culture media on tryptophan oxidation of a monoclonal antibody through gene expression analyses. *Biotechnol J*. 2018;13(10):e1700254.
- Handlogten MW, Wang J, Ahuja S. Online control of cell culture redox potential prevents antibody interchain disulfide bond reduction. *Biotechnol Bioeng*. 2020;117:1329-1336.
- Radhakrishnan D, Robinson SA, Ogunnaike AB. Controlling the glycosylation profile in mAbs using time-dependent media supplementation. *Antibodies*. 2018;7(1):1.
- Yun Z, Takagi M, Yoshida T. Combined addition of glutathione and iron chelators for decrease of intracellular level of reactive oxygen species and death of Chinese hamster ovary cells. *J Biosci Bioeng*. 2003;95(2):124-127.
- Mohammad A, Agarabi C, Rogstad S, et al. An ICP-MS platform for metal content assessment of cell culture media and evaluation of spikes in metal concentration on the quality of an IgG3:kappa monoclonal antibody during production. *J Pharm Biomed Anal*. 2019;162:91-100.
- Xu J, Jin M, Song H, et al. Brown drug substance color investigation in cell culture manufacturing using chemically defined media: a case study. *Process Biochem*. 2014;49(1):130-139.
- Gawlitzeck M, Estacio M, Fürch T, Kiss R. Identification of cell culture conditions to control N-glycosylation site-occupancy of recombinant glycoproteins expressed in CHO cells. *Biotechnol Bioeng*. 2009;103(6):1164-1175.
- Paul BT, Manz DH, Torti FM, Torti SV. Mitochondria and iron: current questions. *Expert Rev Hematol*. 2017;10(1):65-79.

35. Chumsae C, Gifford K, Lian W, Liu H, Radziejewski CH, Zhou ZS. Arginine modifications by Methylglyoxal: discovery in a recombinant monoclonal antibody and contribution to acidic species. *Anal Chem*. 2013;85(23):11401-11409.
36. Ha H, Lee HB. Reactive oxygen species as glucose signaling molecules in mesangial cells cultured under high glucose. *Kidney Int Suppl*. 2000;77:S19-25.
37. Reusch D, Tejada ML. Fc glycans of therapeutic antibodies as critical quality attributes. *Glycobiology*. 2015;25(12):1325-1334.
38. Thomann M, Reckermann K, Reusch D, Prasser J, Tejada ML. Fc-galactosylation modulates antibody-dependent cellular cytotoxicity of therapeutic antibodies. *Mol Immunol*. 2016;73:69-75.
39. Sha S, Agarabi C, Brorson K, Lee DY, Yoon S. N-glycosylation design and control of therapeutic monoclonal antibodies. *Trends Biotechnol*. 2016;34(10):835-846.
40. Liu B, Spearman M, Doering J, Lattová E, Perreault H, Butler M. The availability of glucose to CHO cells affects the intracellular lipid-linked oligosaccharide distribution, site occupancy and the N-glycosylation profile of a monoclonal antibody. *J Biotechnol*. 2014;170:17-27.
41. Gramer MJ, Eckblad JJ, Donahue R, et al. Modulation of antibody galactosylation through feeding of uridine, manganese chloride, and galactose. *Biotechnol Bioeng*. 2011;108(7):1591-1602.
42. McBride HM, Neuspiel M, Wasiak S. Mitochondria: more than just a powerhouse. *Curr Biol*. 2006;16(14):R551-560.
43. Starkov AA. The role of mitochondria in reactive oxygen species metabolism and signaling. *Ann N Y Acad Sci*. 2008;1147:37-52.
44. Fenton HJH. LXXIII.—oxidation of tartaric acid in presence of iron. *J Chem Soc Trans*. 1894;65(0):899-910.
45. Zorova LD, Popkov VA, Plotnikov EY, et al. Mitochondrial membrane potential. *Anal Biochem*. 2018;552:50-59.
46. Chakrabarti L, Mathew A, Li L, et al. Mitochondrial membrane potential identifies cells with high recombinant protein productivity. *J Immunol Methods*. 2019;464:31-39.
47. Hinterkorn G, Brugger G, Muller D, et al. Improvement of the energy metabolism of recombinant CHO cells by cell sorting for reduced mitochondrial membrane potential. *J Biotechnol*. 2007;129(4):651-657.
48. Powell SR. The antioxidant properties of zinc. *J Nutr*. 2000;130(5S Suppl):1447s-1454s.
49. Costa AR, Rodrigues ME, Henriques M, Oliveira R, Azeredo J. Strategies for adaptation of mAb-producing CHO cells to serum-free medium. *BMC Proc*. 2011;5 Suppl 8(Suppl 8):P112.
50. Shridhar S, Klanert G, Auer N, et al. Transcriptomic changes in CHO cells after adaptation to suspension growth in protein-free medium analysed by a species-specific microarray. *J Biotechnol*. 2017;257:13-21.

SUPPORTING INFORMATION

Additional supporting information may be found online in the Supporting Information section at the end of this article.

How to cite this article: Graham RJ, Mohammad A, Liang G, et al. Effect of iron addition on mAb productivity and oxidative stress in Chinese hamster ovary culture. *Biotechnol Progress*. 2021;37(5):e3181. <https://doi.org/10.1002/btpr.3181>